9. Krautler, B.; Bard, A. J. J. Am. Chem. Soc. **1978**, 100, 4317.
10. Duonghong, D.; Borgarello, E.; Grätzel, M. J. Am. Chem. Soc. **1981**, 103, 4685.
11. Kuczynski, J.; Thomas, J. K. Chem. Phys. Letts. **1982**, 88, 445.
12. Kuczynski, J.; Milosavljevic, B. H.; Thomas, J. K. J. Phys. Chem., in press.
13. Kuczynski, J. P.; Milosavljevic, B. H.; Thomas, J. K. J. Phys. Chem. **1983**, 87, 3368.
14. Farrington, J. A.; Ebert, M.; Land, E. J.; Fletcher, K. B.B.A. **1973**, 314, 372.
15. Patterson, L. K.; Small, R. D.; Scaiano, J. C. Rad. Res. **1977**, 72, 218.
16. Duonghong, D.; Ramsden, J.; Grätzel, M. J. Am. Chem. Soc. **1982**, 104, 2977.
17. Henglein, A. Ber. Bunenges. Phys. Chem. **1982**, 86, 241.
18. Grossweiner, L. S.; Matheson, M. S. J. Phys. Chem. **1957**, 61, 1089.
19. Chandrasekaran, K.; Thomas, J. K. Chem. Phys. Lett. **1983**, 99, 7.

RECEIVED June 8, 1984

Reaction Kinetics as a Probe for the Dynamic Structu of Microemulsions

R. LEUNG, M. J. HOU, C. MANOHAR[1], D. O. SHAH[2], and P. W. CHUN[3]

Departments of Chemical Engineering and Anesthesiology, University of Florida, Gainesville, FL 32611

The coagulation of the hydrophobic AgCl sols has been investigated by stopped-flow method employing microemulsions composed of SDS, IPA, water and benzene as reaction media. Two enhancement peaks of the coagulation rate have been observed. In order to correlate the enhancements with the dynamic structures of reaction media, the physico-chemical properties of the microemulsions have been measured using various techniques including conductance, viscosity, light scattering, ultracentrifuge, ultrasonic absorption and pressure-jump relaxation. Subregions consisting of different microstructures within a clear single microemulsion phase have thus been delineated. Accordingly, the broad enhancement peak of the coagulation of 0.56 water mass fraction is associated with surfactant aggregates in the alcohol-rich solvent. The sharp enhancement peak at 0.855 water mass fraction has been attributed to the fast coagulation of normal micelles leading to micellar growth. It has been found by the titration method that a minimum of eight water molecules per surfactant molecule are required to hydrate the sulfate group for the dissolution of SDS into IPA.

A microemulsion is a thermodynamically stable isotropic dispersion two relatively immiscible liquids, consisting of microdomains of one or both liquids stabilized by a interfacial film of surface-active molecules. In practice, one often identifies the microemulsion by the formation of a clear isotropic mixture of the two immiscible liquids in the presence of appropriate emulsifiers. In a phase diagram, such region is referred as the microemulsion phas It has been shown that microemulsion regions consist of different microstructures (1,2), e.g., water-in-oil (W/O), oil-in-water (O/W

[1]Current address: Chemistry Division, Bhabha Atomic Research Center, Bombay-400085, Indi
[2]To whom correspondence should be addressed.
[3]Current address: Department of Biochemistry and Molecular Biology, College of Medicine, University of Florida, Gainesville, FL 32611

0097-6156/85/0272-0325$06.00/0
© 1985 American Chemical Society

etc. A number of different techniques such as light scattering, neutron-scattering, ultrasonic absorption, ultracentrifugation, as well as relaxation measurements have been used to characterize different microstructures within a single phase microemulsion region (1-12). The presence of different microstructures in reaction media can affect the mechanism and rate of a chemical reaction. Therefore, kinetics of a chemical reaction can be used as a probe for investigating the transition of the microstructure within a single phase microemulsion region. As a matter of fact, the microemulsions, being transparent, are very suitable systems for monitoring the chemical reactions spectrophotometrically.

Silver chloride precipitation is one of the most extensively investigated reactions due to its importance in photographic industry (13-22). Aqueous suspension of silver halide in the presence of protectice colloid such as gelatin, surfactants, is usually called emulsions in photography. The turbidity measurement is conventionally used to monitor the precipitation process. It is well-known that the turbidity of the aqueous solution increases rapidly upon mixing silver nitrate with alkali halid in the absence of protective colloids. Matijevic and Ottewill (13,14) have attributed such turbidity enhancement to the fast coagulation and precipitation of silver halide sols. They investigated the effect of cationic detergents on the stability of negatively-charged silver halide sols. Periodic "sensitized" coagulation and stabilization regions of the sols were observed upon increasing the detergent concentration. When the detergent concentration approached its critical micelle concentration, the detergents acted as protective colloids and the coagulation rate of silver halide sols was drastically reduced. In another set of studies on the stability of positively charged silver halide sols in the presence of anionic surface active agents, Ottewill and Watanabe (15) have shown that the stability of the sols decreased initially (coagulated faster) and then increased again up to a limiting value due to the adsorption of surface active molecules on the sols. A theory has also been proposed to account for these experimental findings (14,15).

In this preliminary study, we have investigated the coagulation rate of silver chloride sols in microemulsion media. The results are intimately related to structural properties of the microemulsions.

Experimental

Materials and Methods. The sodium dodecyl sulfate (SDS) was of purity higher than 99% from BDH. $AgNO_3$, NaCl were ACS certified grade from Fisher Scientific Company. Isopropyl alcohol (IPA) and benzene were of 99% purity from Fisher Scientific Company. All chemicals were used as received without further purification.

The viscosity was measured by Cannon-Fenske viscometer (#100). Light scattering was monitored by Duophotometer Model 5200 (Wood Mfg. Co.). The ultrasonic absorption was measured using Matec Pulse Modulator and Receiver model 6600. Pressure-jump studies were performed using DIA-LOG system with conductivity detection. The stopped-flow experiments were carried out using Durrum Model D-115 systems. The ultracentrifuge studies were carried using a Beckman Model E analytical ultracentrufuge with Schlieren optics. All the measurements were carried out at 25°C.

Preparation of AgCl Sols. Two stock aqueous solutions of 5 mM $AgNO_3$ and of 5 mM NaCl were first prepared separately. Microemulsions were then prepared by mixing specific amount of SDS, IPA, benzene and either one of the two aqueous stock solutions so that two identical microemulsion samples at a desired composition were formed except one contained $AgNO_3$ and the other contained NaCl. Using stopped-flow apparatus, the AgCl sols were formed upon a rapid injection of these two identical microemulsion samples into a mixing chamber. The turbidity development through the coagulation of the AgCl sols was then followed by transmittance measurement.

Coagulation Rate Measurements. As shown by Matijevic and Ottewill (13), the turbidity τ resulting from the formation of the solid phase in a solution can be defined by the relation:

$$I = I_0 e^{-\tau l} \tag{1}$$

where I_0 and I are the intensities of the incident and transmitted radiation respectively, and l is the optical path length of the cell employed. For small particles ($r < \lambda/20$) in the absence of consumptive light absorption, τ is related to the number of particles per milliliter N_p, and their individual volume V_p by Rayleigh equation, viz.,

$$\tau = A\, N_p V_p^2 \tag{2}$$

here A is an optical constant given by:

$$A = \frac{24\pi^3 n_0^4}{\lambda^4} \left(\frac{n^2 - n_0^2}{n^2 + 2n_0^2}\right)^2 \tag{3}$$

where n_0 is the refractive index of the solvent while n is the refractive index of the particles. λ is the wavelength of the light used (in vacuo).

For a coagulation process, the change of turbidity with time is given by the equation,

$$\tau = A\, N_p V_p^2 (1+kt) \tag{4}$$

where k is a rate constant. When the particles are small enough to obey Rayleigh's equation (2), a linear relationship between turbidity and time is obtained (13).

For all samples studied, the use of initial coagulation rate (the first 2 seconds in a overall process longer than 100 seconds) does provide a linear (or pseudo-linear) rate constant k for comparative purpose. Moreover, the use of initial coagulation rate for comparison is justified in view of the fact that the concentration product of AgCl in our samples is considerably greater than the solubility product (1.765×10^{-10} at 25°C) and hence, upon mixing, the nuclei of AgCl are formed spontaneously without significant induction-time delay. However, due to the possible complication involved in the multicomponent systems, we report all our initial coagulation rates in terms of a relative rate constant k_{rel} using pure water as a reference,

$$k_{rel} = \frac{k \text{ in microemulsion media}}{k \text{ in pure water}} \quad (5)$$

Assuming the changes of A and V_p on various microemulsion media are negligible, and N_p is proportional to the volume fraction of water in a microemulsion sample, the following equation is then used to obtain a relative rate constant for a microemulsion sample,

$$k_{rel} = \frac{\left[\frac{1}{N_p}\frac{d\ln(I/I_0)}{dt}\right]_{microemulsion}}{\left[\frac{1}{N_p}\frac{d\ln(I/I_0)}{dt}\right]_{water}} \quad (6)$$

Results and Discussions

Coagulation of Hydrophobic AgCl Sols. The experimental line along which all the measurements were made in a microemulsion phase is shown in Figure 1. The phase diagram for IPA + SDS + benzene + water system was obtained by Clausse (23). The mass ratio of SDS/IPA is 0.5 throughout the phase diagram, and the mass ratio of benzene/SDS is 0.33 for all the samples studied. The structure of the microemulsions employed as reaction media may differ markedly from alcohol-rich (point A) to water-rich (point B) region in the phase diagram. Figure 1 shows the variation of relative rate constant as a function of mass fraction of water in microemulsions. The enhancements in the coagulation rate at specific water mass fractions of 0.56 and 0.855 are quite striking. Of the two enhancement peaks observed, the highest peak at 0.855 mass fraction of water is very narrow and intense, while the other peak at 0.56 is broad but less intense. The former does not seem to be related to the formation of micelles because the surfactant concentration is about 15 times higher than the critical micelle concentration. The broadness of the latter peak is indicative of a certain structural property that may persist in a wide range of alcohol-rich region of the microemulsion phase.

It is of interest to note the resemblance of our data to that reported by Friberg et al. (24). They have investigated the rate of hydrolysis of p-nitrophenol laurate in the microemulsion system consisting of ceryltrimethyl ammonium bromide, butanol and water. Two pronounced and broad peaks of the reaction rate were observed. The enhancements have been ascribed to the conventional micellar catalysis effect in which the micellar surface charge density plays a dominant role. However, this seems unlikely to be the reasons for the enhancements observed in our studies in view of the sharpness of the peak at 0.855 as compared to that reported by Friberg et al. (24).

We will discuss first the reaction kinetics by which the turbidity increases. As shown by Ottewill and Watanabe (15) in the case of sol formation, a complex series of consecutive and simultaneous reactions occur. These can be schematically presented as follows (15):

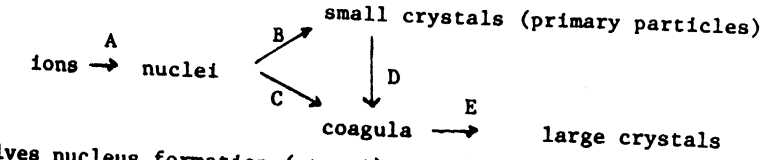

It involves nucleus formation (step A), crystal growth (step B) and coagulation (step C and D) of primary particles. The turbidity development observed in our experiments can not be related to the reaction A because the nucleus formation is usually very fast at reasonably high supersaturation and therefore will terminate before experimental observations are recorded. Another supporting evidence is that the nuclei of AgCl sols may only consist of about five ions as reported by Klein et al. (25). The change in opalescence resulted from such small nuclei is probably not perceivable. Thus, the reactions mostly observed in the experiments would appear to be B, C and D.

In many classical coagulation studies using performed sols (14, 15) with the addition of coagulatory agent (such as surface active molecules), a simplified analysis is feasible in which the growth of nuclei to primary particles is very rapid, and hence the reaction observed is predominantly the coagulation of the primary particles, i.e. the reaction D. This reaction has been found to depend strongly on the surface potential of the sol particles. The adsorption of surface active agents on sols may modify the surface potential and consequently alter the coagulation rate. In our studies, we have chosen a different approach, namely by monitoring the formation of hydrophobic sols in statu nascendi (13) using microemulsions as reaction media. The analysis thus appears complicated due to the possible influences of the microemulsions on the nucleation and crystal growth. Some of these influences are even not clear at present. It is our opinion, however, that the surface potential of the sols and the nature of the media are principally the controlling factors in the crystal growth and coagulation process.

Physico-Chemical Properties of the Microemulsions. In order to delineate the correlation between the coagulation rate and the dynamic structure of microemulsions, we have performed a number of measurements to determine various physico-chemical properties of the microemulsion phase along the experimental line. Figure 2 shows the conductance of the microemulsions. The maximum conductance around 0.56 water mass fraction corresponds to the peak of the coagulation rate in Figure 1. The increasing conductance with the addition of water in the alcohol-rich region may be attributed to the increased ionization of SDS molecules. The decreasing conductance beyond the maximum is presumably due to the dilution effect on the conductance by additional quantity of water.

Figure 3 represents the plot of viscosity vs. water content. It shows that as the amount of water decreases, the viscosity increases up to a water mass fraction of 0.56, and with further reduction in water content there is no significant change in viscosity. The decrease in viscosity in the region of water mass fraction greater than 0.56 is consistent with the dilution effect shown in the electrical conductivity measurements (Figure 2).

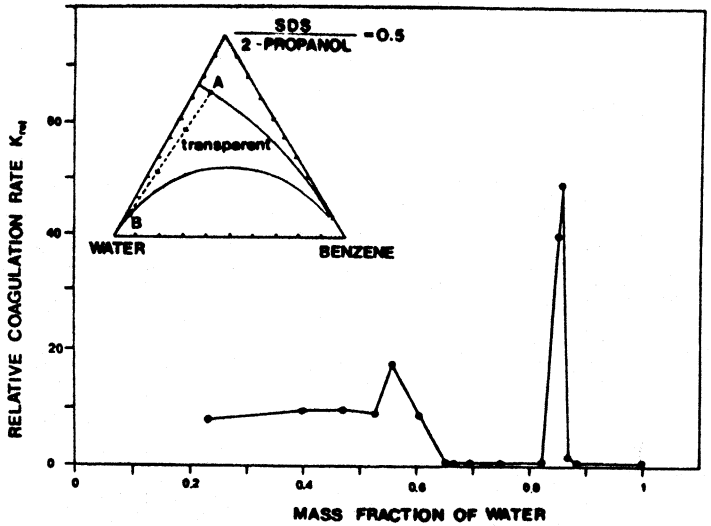

gure 1. Variation of the relative coagulation rate constant k_{rel} of AgCl sols as a function of water content along the experimental line AB in the phase diagram of SDS-IPA-benzene-water microemulsions.

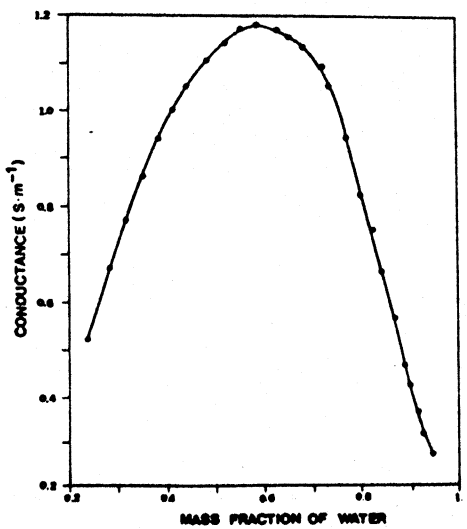

gure 2. Electrical conductance as a function of water mass fraction along the line AB (Figure 1) of SDS-IPA-Benzene-Water microemulsion system.

In order to further understand the association structure of the surfactant in the solution, we have measured the light scattering as shown in Figure 4. Interestingly, the results exhibit two peaks corresponding to the peaks of the coagulation rate in Figure 1. The broad peak in Figure 4 also bears a strong resemblance to the results reported by Friberg et al. (24). It can be stated from these results that starting from the alcohol-rich region, the addition of water in microemulsions results in certain association structure which enhances the light scattering from the solution. Similar conclusions have also been drawn by Sjoblom and Friberg (10) for water, pentanol, potassium oleate and hydrocarbon oil microemulsion systems. The association structure of the surfactant in the alcohol-rich region may resemble the water-in-oil (W/O) microemulsions (10).

It should be noted that a concentration fluctuation can also increase the light scattering intensity by orders of magnitude near the vicinity of a critical point. It is well established from recent studies (26-30) that a critical-like behavior has been observed near the percolation threshold in a W/O microemulsion system where a strong concentration fluctuation occurs due to the long range van der Waals interaction force between the microemulsion droplets. However, at present we do not have any experimental evidence to distinguish between the micellar growth and concentration fluctuation mechanism to explain the light scattering data. It is to be noted that a sharp peak in light scattering around 0.855 water mass fraction indeed is observed. A broad and smooth transition zone has been observed in the transition of spherical to rod (cylindrical) shape of micelles using viscosity, light scattering and magnetic field measurement (31,32). It is likely, therefore, that this sharp peak may not be related to a structural transition, but a concentration fluctuation which we will discuss in more details later.

Besides the light scattering data, the ultracentrifugation results further confirm the existence of surfactant aggregates in this system (Figure 5). For the samples with 0.855 water mass fraction or greater, no sedimentation peak was observed. We had expected that normal SDS micelles with solubilized benzene may exist in this region. The absence of the sedimentation peak is probably due to the electric repulsion force between the micelles. This is consistent with the observation that no sedimentation peak was observed in a pure 0.5 M SDS aqueous solution containing normal micellar aggregates. For the solutions with water fraction 0.8 down to 0.25, sedimentation peaks were observed and the sedimentation coefficients shown in Figure 5 were calculated from the velocity of the sedimenting peaks (33-35). As seen in Figure 5, the change of sedimentation coefficients with rotor speed was unexpected. It suggests that the aggregates of the surfactant are rather fragile and sensitive to the centrifugal force. The increase in the value of sedimentation coefficient as the amount of water decreases does not necessarily indicate the growth of aggregates. It may also be attributed in part to the decreasing buoyancy of the solvent due to the continuous addition of IPA into solutions. Further attempts to obtain the particle size from the sedimentation coefficient is thus thwarted due to the constant variation in the composition of the continuous media. For the solutions with water fraction less than 0.25, no sedimentation peak was observed.

Figure 6 represent various Schlieren patterns of the samples of different compositions. The Schlieren peak appears upward if the re-

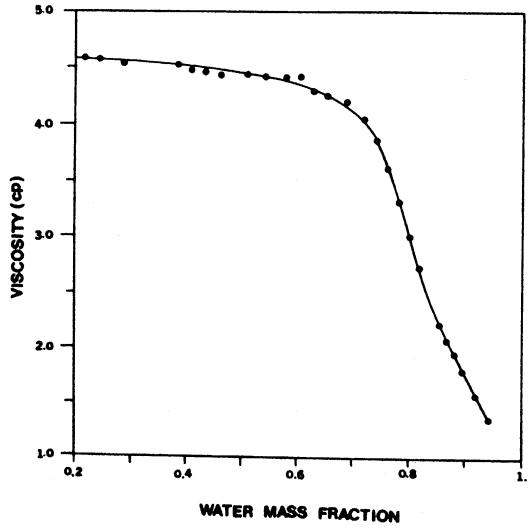

Figure 3. Viscosity as a function of water mass fraction along the line AB (Figure 1) of the SDS-IPA-Benzene Water microemulsion system.

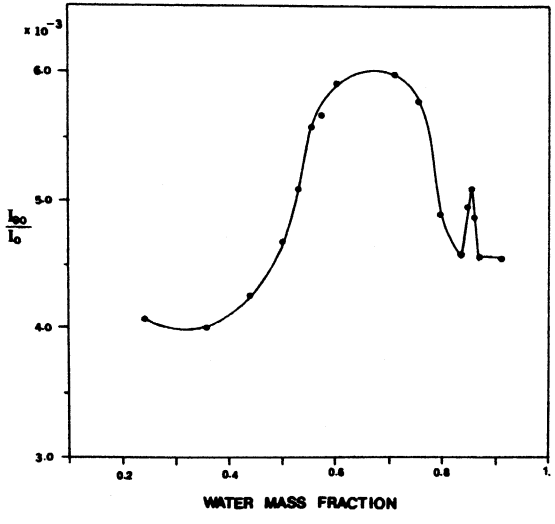

Figure 4. Ratio of light scattering intensity I_{90}/I_0 as a function of water mass fraction along the line AB (Figure 1) of the SDS-IPA-Benzene-Water microemulsion system.

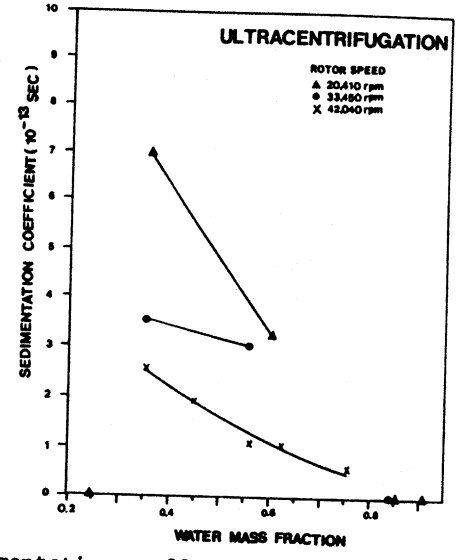

Figure 5. Sedimentation coefficients at various rotor speeds as a function of water mass fraction along the line AB (Figure 1) of the SDS-IPA-Benzene-Water microemulsion system.

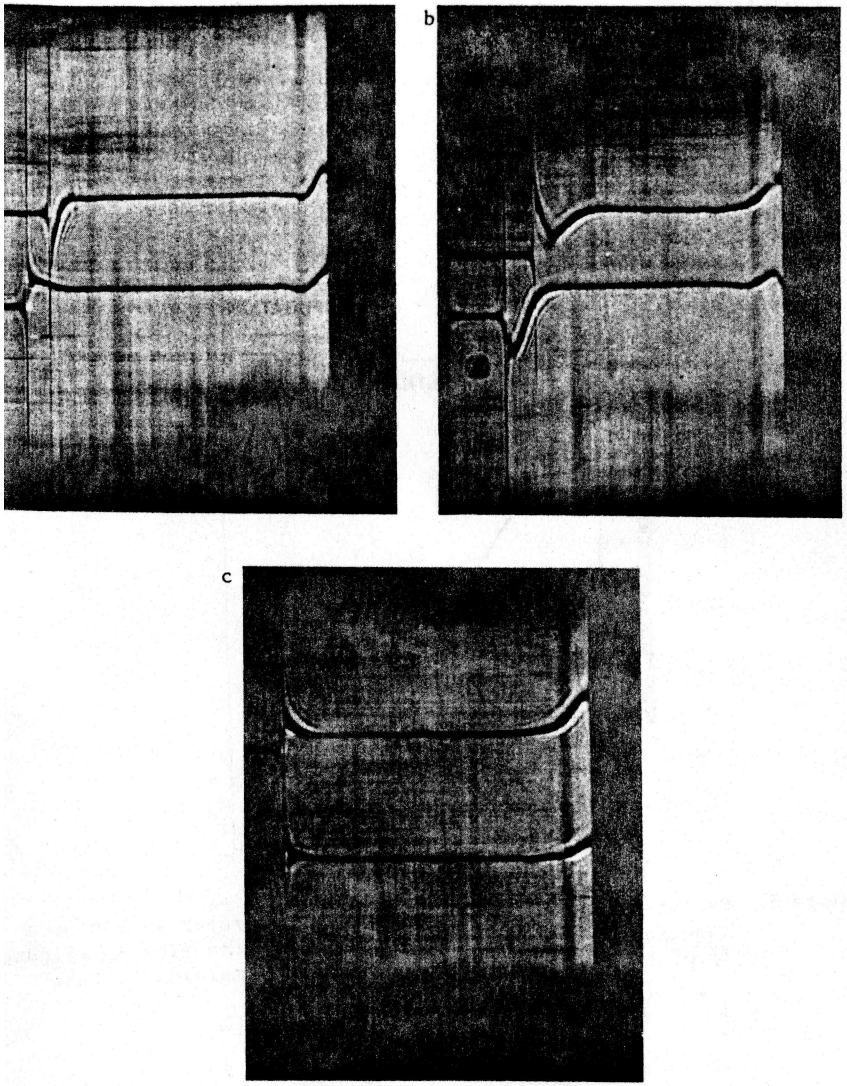

igure 6. Ultracentrifuge Schlieren patterns of the microemulsions
long the line AB in Figure 1. Note the left hand side is the menis-
us, and the right hand side corresponds to the bottom of the cell.
a) Upper curve corresponds to the sample at 0.8 water mass fraction,
ower curve to the sample at 0.853 water mass fraction; 1651 sec
lapsed after reaching the speed of 33,350 rpm.
b) Upper curve corresponds to the sample at 0.35 water mass fraction,
ower curve to the sample at 0.567 water mass fraction; 2595 sec
lapsed after reaching the speed of 42,040 rpm.
c) Upper curve corresponds to the sample at 0.24 water mass fraction,
ower curve to the sample at 0.908 water mass fraction; 1377 sec
lapsed after reaching the speed of 20,410 rpm.

fractive index increment is positive, dn/dc>0; and downward if negative, dn/dc<0, where n denotes the local refractive index of the solution and c is the local solute concentration in the solution (33-35). Figure 6(a) shows an upward meniscus boundary for the sample of 0.853 water mass fraction (lower curve) and a downward peak for the sample of 0.8 water mass fraction (upper curve). It is evident that an inversion of the refractive index increment dn/dc occurs in the region of water fraction between 0.85 and 0.8, indicating a change in the solution properties. Such inversion is also accompanied with the onset of the sedimentation of aggregates. Figure 6(b) indicates the sedimentation peaks observed at 0.567 (lower curve) and 0.35 (upper curve) water fraction. Both peaks are downward. It is noteworthy that there exists another upward peak near the bottom of the cell for both samples. This peak appears to float up against the centrifugal field during the course of centrifugation. The reason for this floating peak is not clear at present. However, it can not be attributed to the flotation of the aggregates because a flotation peak usually appears downward (with negative refractive index increment). We propose that this peak may be related to the compressibility of the system for which the aggregates under compression tend to relax back through a back-diffusion of the solutes against the centrifugal field (36). Figure 6(c) represent the Schlieren patterns of the sample at 0.24 water fraction. No sedimentation peak was observed and the meniscus boundary was inverted from downward to upward again, indicating the occurrence of a structural transition (phase separation occurs at composition A, Figure 1).

The ultrasonic absorption of the solutions at 5MHz also corroborates the picture that emerges from the ultracentrifugation results; Fig. 7. The maximum absorption observed at 0.56 water fraction corresponds to the peak of light scattering and coagulation rate of AgCl, and is indicative of the ease of perturbation of the structures by the ultrasonic pressure. The processes to which the ultrasonic relaxation of surfactant solutions can be attributed are: (1) the exchange of alcohols between the mixed micelles and surrounding solution; (2) the exchange of surfactants between the micelles and surrounding solution; (3) the ion association-dissociation equilibrium of the electrolytes; and (4) concentration fluctuation of the solution. Zana et al. (28) have investigated the ultrasonic absorption behavior in many W/O microemulsion systems. It was found that the high ultrasonic absorption could only be detected if large concentration fluctuations occurred in the system. Hence, the first and second process can be excluded. The third process is also unlikely to be the cause for the maximum absorption in view of the results reported by Friberg et al. (24) that a continuous increase of ^{81}Br line width occurs as the water content decreases. The broadening of ^{81}Br line width indicates the increasing strength in the counter-ion binding. The ultrasonic absorption, if any, will then appear as a monotonic function, instead of a maximum. We shall therefore only consider the concentration fluctuation as the probable cause of absorption maximum.

The concentration fluctuations in our system can possibly further be subdivided into a solute (surfactant aggregates) concentration fluctuation and a solvent concentration fluctuation. The solute concentration fluctuation is similar to that of critical-like behavior observed in many W/O microemulsion systems (28), while the solvent

concentration fluctuation may result from the mixed solvent of IPA and water. It has been reported (37) that a maximum ultrasonic absorption occurs at 0.84 mass fraction of water (mole fraction of IPA is 0.057) in a IPA + water mixture. A shift in the composition of this maximum absorption may occur upon addition of other additives. Therefore, we can not rule out the solvent concentration fluctuation as a possible cause of the maximum absorption.

We have also performed a pressure-jump relaxation study on the system in an attempt to directly probe the microstructures in our system. It is now well established that the existence of normal micellar structures gives rise to two well separated relaxation processes (38-40). The fast relaxation process with relaxation time τ_1 in micro-seconds range is related to the fast exchange of surfactant monomers between the micelles and the surrounding solution. The slow relaxation process with relaxation time τ_2 in milli-seconds range is associated with the micellar formation-dissolution equilibrium. No experimental data have yet been reported regarding the pressure-jump relaxation in a reverse micellar system. In the water-rich region (water mass fraction greater than 0.75) of our microemulsion system, the relaxation spectra resemble to that of normal micelles except that there exists an extra slow relaxation process (referred as τ_{slow}). τ_1 is too fast to measure by pressure-jump apparatus. The value of τ_2 as plotted in Figure 8 is smaller than that of pure SDS micelles (800 milliseconds to 5 seconds) in the same SDS concentration range of 100 to 200 mM by Kahlweit (38). This may be attributed to the presence of short chain alcohol (39). We have also shown in a recent study (41) that the addition of a short chain alcohol (propanol) increases the rate of micelle formation-dissolution significantly. The amplitude of τ_{slow} process in the water-rich region is very small and hence the resolution of relaxation time τ_{slow} is poor. Within the range of experimental accuracy, τ_{slow} was found to be independent of the microemulsion composition.

As the amount of IPA and SDS continuously increases in the solution, the relaxation spectra seem to undergo a smooth transition. The amplitude of τ_{slow} process is gradually increasing, while the amplitude of τ_2 process is diminishing. We only reported τ_2's for the water rich region in Figure 8 due to the poor resolution of τ_2 with increasing alcohol concentration. However, the value of τ_2 appears to increase with alcohol concentration and approach a plateau value around 0.8 sec at alcohol-rich corner. We should note that τ_{slow} is probably not related to micelle formation. We have attributed these slow processes to the compressibility of the IPA + water solvent in our recent study (41). We have shown (41) that a mM potassium chloride in a mixed IPA + water solvent gives rise to a similar relaxation signal (consisting of three relaxation processes and relaxation times to that of the sample at 0.24 water mass fraction. It is obvious that the signal resulted from the relaxation of normal micelles dominates the relaxation spectra in the water-rich region and hence the amplitude of τ_{slow} process is small. But as the alcohol concentration increases, the normal micellar aggregates disappear gradually and a structural transition takes place. The relaxation spectra will then be overshadowed by the relaxation of the mixed solvent of IPA + water. The mechanisms corresponding to this mixed solvent relaxation are not established at present.

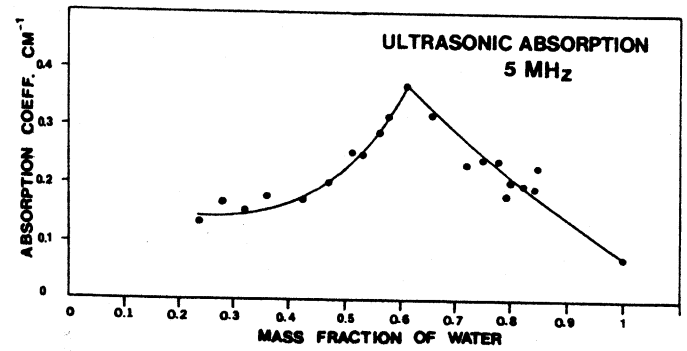

Figure 7. Ultrasonic absorption as a function of water mass fraction along the line AB (Figure 1) of the SDS-IPA-Benzene-Water microemulsion system.

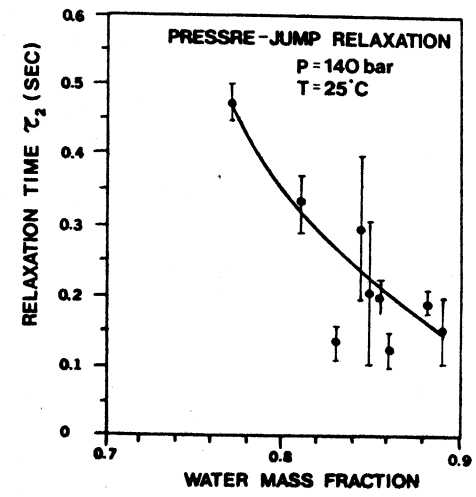

Figure 8. Variation of relaxation time τ_2 as a function of water mass fraction.

Piecing together all the experimental data we have thus far ented, we can attain the following sketch regarding the structural erties of our microemulsion system. The sedimentation studies irm the existence of association structures of surfactants in alcohol-rich region. Based upon the light scattering data ıre 4) we can state that the addition of water induces the ciation of the surfactants starting at about 0.4 water mass frac- . Between 0.56 to 0.7 water fraction, the surfactant aggregates concentration fluctuation may coexist in the system. The associa- structures over the alcohol-rich region should resemble the in- ed micelles or W/O microemulsions. Beyond 0.7 water mass frac- , a structural transition from inverted to normal micellar ctures occurs and hence the light scattering decreases. If the al micellar structure persistently exists over the alcohol-rich on, we would have expected that the value of τ_2 decreases con- ously instead of increases according to the relaxation study of concentration SDS solution reported by Kahlweit (38).

The structural studies reported by Bellocq et al. (5,6) on the oemulsion system composed of SDS, butanol, water and toluene can eferred to support the types of association structures mentioned e. Three subregions consisting of different microstructures in a le microemulsion phase region have been identified using quasi- tic Rayleigh scattering. In view of the striking resemblance of phase diagram reported by Bellocq et al. (5,6) to ours, similar lusions can also be drawn for our system. The formation of rical inverted structures are responsible for the light scatter- enhancement starting at 0.4 water fraction as shown in Figure 4. s noteworthy that the light scattering intensity remains constant further increasing the water fraction from 0.56 to 0.7. This ests that the additional water does not induce further growth nverted micelles, but partition in the continuous medium. This only explains the decrease of the conductance beyond the 0.56 r mass fraction, but also indicates that large micellar struc- s are not formed in the IPA + water solvent. Hence, the concen- ion fluctuation may play an important role in light scattering. can explain the fact that the association structures in the al- l-rich region are not rigid. They are fragile and easy to per- as concluded from the ultracentrifuge study.

The structural transition from inverted to normal micellar struc- occurs around 0.8 to 0.7 water mass fraction. It is obviously ogressive transition. The microstructure in this region is not well established. The ultracentrifuge study has shown that the rted micellar structure may exist persistently down to 0.8 water fraction. But the quasielastic light scattering has detected trace of normal micellar structure as low as 0.7 water mass tion (5).

Lastly, we would like to point out that the head group of the c surfactant have to be hydrated by a minimum amount of water rder to dissolve into a low polarity solvent (e.g. short chain hols). In the hydrocarbon oil rich corner of a microemulsion e diagram, micellization occurs as long as the minimum water re- ed to hydrate the ionic head group is added (5). Hence the mini- water to surfactant molar ratio required for such hydration can be rmined by light scattering measurement. The ratio has been d to be 10 for sulfate surfactants in toluene and 8 for carboxy-

late surfactants in dodecane (5). But in the alcohol (short chain) rich corner, the micellization does not occur upon the addition of necessary minimum amount of water. Therefore the light scattering measurement cannot be used to determine the minimum water required. Instead, we have developed a titration method for this purpose. Starting from the surfactant-rich region of our system, the added water is expected to partition in both surfactant phase (hydration) and continuous medium (IPA). Then the total number of water molecules N_w added to the solution is:

$$N_w = N_w^s + N_w^a \tag{7}$$

where N_w^s denotes the number of water molecules that hydrate the surfactant head groups, and N_w^a is the number of water molecules partitioning in the IPA. Assuming h is the minimum number of water molecules per surfactant molecule required for hydration, we then have:

$$N_w^s = hN_s \tag{8}$$

where the N_s is the total number of surfactant molecules in the solution. We can also express the N_w^a as:

$$N_w^a = kN_a \tag{9}$$

where k is the proportional constant of water molecules partitioning in the IPA, and N_a is the total number of alcohol molecules in the solution. Combining the equation (7), (8) and (9) gives:

$$\frac{N_w}{N_s} = k\frac{N_a}{N_s} + h \tag{10}$$

We took a clear microemulsion sample of 0.22 water mass fraction near the phase boundary, first titrated with IPA till the sample just became turbid, then titrated with water till the sample became clear again. Repeating these procedures many times and plotting the ratio of N_w/N_s versus N_a/N_s, we then obtained a straight line as shown in Figure 9. The slope yields the constant k and the intercept on y-axis corresponds to the minimum number of water molecules per surfactant molecule required for dissolution. It was concluded that minimum 8 water molecules are needed to hydrate each sulfate group for dissolution of SDS into IPA. It should be noted that this titration method can only be used in the miscibility range of the short chain alcohol with water.

Interrelationship Between the Reaction Kinetics and the Dynamic Structure of Microemulsions. We now come to our final goal to correlate the reaction kinetics with the dynamic structures of the microemulsions. The coagulation rate of AgCl sols depends on the surface charge of the sols. High surface charge density prevents the collisions of the preliminary particles of AgCl crystals, and consequently results in the slow coagulation rate and small size of precipitates. The enhancement of the caogulation in Figure 1 from water mass fraction of 0.22 to 0.65 corresponds to the region where the nature of the continuous phase of the microemulsions is dominated

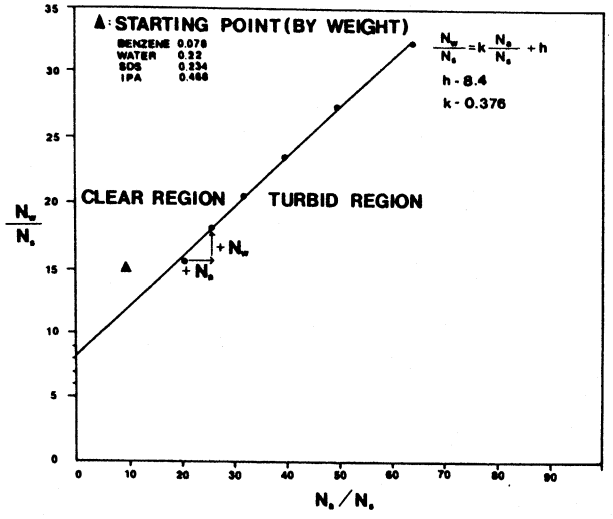

Figure 9. Minimum number of water molecules, h, per surfactant molecule needed to hydrate the sulfate group for the dissolution of SDS into IPA.

by alcohol (low polarity). The association structures in this region are probably inverted micelles.

It has been shown that the stability of colloidal suspensions can also be influenced by a pure alcohol-water mixture, without the addition of any surface active agent. In a study of the flocculation of polystyrene emulsions in ethanol-water mixtures (42), the concentration of sodium chloride required to produce rapid flocculation increases with increasing ethanol concentration up to 0.09 molar fraction, beyond this composition, the concentration of sodium chloride required for flocculation decreases rapidly. It will be very informative, therefore, to compare our coagulation rate obtained in the microemulsion media to that in pure IPA + water mixture. The results can be used to further delineate the role of inverted micellar structure on the enhancement of coagulation.

The reasons for the sharp peak of coagulation rate at 0.855 water fraction can be explained as follows. The sharp increase in the coagulation rate is presumably due to the fast mutual coagulation of the normal micelles as a result of increasing concentration of SDS. Many facts substantiate this conjecture. Using density and heat capacity measurements, Roux et al. (7,8) have found that the micellar growth starts at about 0.8 water mass fraction along a dilution line (by water), and at about 0.85 water mass fraction along the lower demixing line in a microemulsion system consisting of SDS, butanol, water and toluene. The discrepancy in these two water fractions appears to result from the micelles swollen by the solubilized toluene along the lower demixing line. In view of the striking similarity in the phase diagram of our microemulsion system with that of Roux et al., it is plausible to propose that the micellar growth occurs at 0.85 water mass fraction in our systems.

We would like to point out that this micellar growth is probably not the type of transition from spherical to cylindrical micelles as usually observed in a concentrated surfactant solution (31,32). A tighter packing micelle is usually expected as a result of this transition. But in contrast, Roux et al. (7,8) have found that a less structured micelle results after the micellar growth. Two counter-acting forces may exist during the course of this micellar growth; one force tends to increase the micellar size due to the continuous increase of SDS concentration, while the other tends to break down the micelles due to the increasing concentration of alcohol (43-45). It is likely due to these counter-balancing forces, that the micellar growth in these microemulsion systems differs from that of sphere to cylinder transition.

It is generally considered that the micelle formation represents a step-wise association process (40). For an ionic surfactant system at low concentration, the mutual coagulation between the micelles is forbidden due to the electrostatic repulsion force. Hence, the micelles grow only by incorporation of monomers only. However, a recent review paper by Kahlweit (38) indicates that at high counter ion concentrations (i.e. high surfactant concentration), the micelles can grow through a bypass of a reversible coagulation of submicellar aggregates. For SDS micellar solution, such bypass coagulation occurs at the concentration of about 200 mM which corresponds to the minimum of $1/\tau_2$. The concentration of SDS at 0.855 water mass fraction of our microemulsion system is about 150mM. We propose that a mutual coagulation of micelles may occur due to the micellar

growth at 0.855 water mass fraction, if taking into account that the presence of IPA may decrease the surface charge density of the micelles. This can explain the occurrence of the sharp light scattering peak at 0.855 water mass fraction in Figure 4. This light scattering peak is due to the concentration fluctuation resulting from the mutual coagulation of micelles.

The sharp enhancement in the coagulation of AgCl sols at 0.855 water mass fraction is the consequence of this mutual coagulation of the micelles. It is likely that the primary particles of AgCl sols are located in the micelles (14) or adsorbed at micelle surface. The electrostatic repulsion force prohibits the coagulation of the micelles, hence the growth of the particles is slow and the size of the precipitate is small in the water-rich region as compared to alcohol-rich region. Our preliminary study on the particle size using scanning electron micrographs indeed confirms that the particles precipitated in the water-rich region is much smaller than in the alcohol-rich region. However, at the composition of micellar growth, the rate of particle growth is enhanced through a fast coagulation of the micelles. The sharpness of the coagulation peak suggests that the micellar growth is only limited to a very finite composition range.

Conclusions

The coagulation of the hydrophobic AgCl sols has been investigated using microemulsions as reaction media. Both equilibrium and dynamic studies have been carried out to delineate the microstructures in a single microemulsion phase. The existence of different microstructures in the single phase region has been established. For the microemulsions with water mass fraction of 0.4 to 0.56, inverted micellar structures are formed. The concentration fluctuation of these inverted micelles may also play an important role in the region from 0.4 to 0.7 water mass fraction. For the microemulsions with water fractions greater than 0.8, the existence of normal SDS micelles have been indicated. It has been shown that the kinetics of the chemical reaction is intimately correlated with the structures and the nature of the medium in the microemulsion phase. Hence, the chemical reaction can serve as a useful approach for probing the dynamic structures in microemulsions. Besides the kinetics of reactions, the morphology of the products from the chemical reaction is also influenced by the microemulsion. This study is thus relevant to various technological applications such as the manufacturing of photographic films (46), catalysis (47) and in general, fine powder technology.

Acknowledgments

We are grateful to the National Science Foundation (Grant No. NSF-CPE 8005851) and the American Chemical Society Petroleum Research Fund (Grant No. PRF-14718-AC5) for supporting this research. We thank Professor M. Clausse at the University of Pau, France, for many stimulating discussions and suggestions.

Literature Cited

1. Clausse, M., Peyrelasse, J., Heil, J., Boned, C., Lagourette, B., Nature, 293, 636 (1981)
2. Boned, C., Clausse, M., Lagourette, B., Peyrelasse, J., McClean, V.E.R., Sheppard, R.J., J. Phys. Chem., 84, 1520 (1980).
3. DeGennes, P.G., Taupin, C., J. Phys. Chem., 86, 2294 (1982).
4. Dvolaitzky, M., Guyot, M., Lagues, M., Le Pesant, J.P., Ober, R., Sauterey, C., and Taupin, C., J. Phys. Chem., 69, 1 (1978).
5. Bellocq, A.M. Fourche, G., J. Colloid Interf. Sci., 78, 275 (1980).
6. Bellocq, A.M., Biais, J., Clin, B., Lalanne, P., and Lemanceau, B., J. Colloid Interf. Sci., 70, 524 (1979).
7. Roux, A.H., Roux-Desgranges, G., Grolier, J.P.E., and Viallard, A., J. Colloid Interf. Sci., 84, 250 (1981).
8. Roux-Desgranges, G., Roux, A.H., Grolier, J.P.E., and Viallard, A., J. Colloid Interf. Sci., 84, 536 (1981).
9. Roux-Desgranges, G., Roux, A.H., Grolier, J.P.E., and Viallard, A., J. Solution Chem., 11, 357 (1982).
10. Sjoblom, E., and Friberg, S., J. Colloid Interf. Sci., 67, 16 (1978).
11. Lindman, B., Stilbs, P., and Moseley, M.E., J. Colloid Interf. Sci., 83, 569 (1981).
12. Tondre, C. and Zana, R., J. Dispersion Sci. Techn., 1, 179 (1980).
13. Matijevic, E. and Ottewill, R.H., J. Colloid Interf. Sci., 13, 242 (1958).
14. Ottewill, R.H., Rastogi, M.C., and Watanabe, A., Trans. Faraday Soc., 56, 855-891 (1960).
15. Ottewill, R.H., and Watanabe, A., Kolloid Z., 170, 38 (1960); Kolloid Z., 170, 132 (1960); Kolloid Z., 171, 33 (1960); Kolloid Z., 173, 7 (1960).
16. Horne, R.W., Matijevic, E., Ottewill, R.H., and Weymouth, J.W., Kolloid Z., 161, 50 (1958).
17. Tezak, B., Matijevic, E., and Schulz, K., J. Colloid Interf. Sci., 55, 1557-1576 (1951).
18. Davies, C.W. and Jones, A.L., Faraday Soc. Discussions, 5, 103 (1949).
19. Davies, C.W. and Jones, A.L., Trans. Faraday Soc., 51, 812-829 (1955).
20. Howard, J.R., Nancollas, G.H., and Purdie, N., Trans. Faraday Soc. 56, 278 (1960).
21. Ohyama, Y. and Futaki, K., Bull. Chem. Soc. Jpn., 28, 243 (1955).
22. Ohyama, Y. and Futaki, K., Bull. Chem. Soc. Jpn., 31, 10 (1958).
23. Clausse, M., private communication.
24. Friberg, S., Rydhag, L., and Lindblom, G., J. Phys. Chem., 77, 1280 (1973).
25. Klein, D.H., Gordon, L., and Walnut, T.H., Talanta, 3, 187 (1959).
26. Cazabat, A.M., Langevin, D., Meunier, J., and Pouchelon, A., Adv. Colloid Interf. Sci., 16, 175-199 (1982).
27. Fourche, G., Bellocq, A.M., Brunetti, S., J. Colloid Interf. Sci., 88, 302 (1982).
28. Zana, R., Lang, J., Sorba, O., Cazabat, A.M., and Langevin, D., J. Physique-Lett., 43, L-829 (1982).
29. Cazabat, A.M., Langevin, D., and Sorba, O., J. Physique-Lett., 43, L-505 (1982).
30. Lagues, M. and Sauterey, C., J. Phys. Chem., 84, 3503 (1980).
31. Porte, G. and Poggi, Y., Phys. Rev. Lett., 41, 1481 (1978).

32. Ekwall, P., Mandell, L., and Solyom, P., J. Colloid Interf. Sci., 35, 519 (1971).
33. Schachman, H.K., "Ultracentrifugation in Biochemistry", Acad. Press, 1959.
34. Freifelder, D., "Physical Biochemistry, Application to Biochemistry and Molecular Biology", W.H. Freeman and Company.
35. Bowen, T.J., "An Introduction to Ultracentrifugation", John Wiley & Sons, (1970).
36. Chun, P.W., Richar, A.J., Herschler, W.P., Krista, M.L., Biopolymers, 12, 1931 (1973).
37. Frank, F., "Water: A Comprehensive Treatise", V. 2, P. 551, Plenum, N.Y. 1973
38. Kahlweit, M., Pure & Appl. Chem., 53, 2069 (1981).
39. Yiv, S. Zana, R., Ulbricht, W., and Hoffmann, H., J. Colloid Interf. Sci., 80, 224 (1981).
40. Aniansson, E.A.G., Wall, S.N., Almgren, M., Hoffmann, H., Kielmann, I., Ubricht, W., Zana, R., Lang, J. and Tondre, C., J. Phys. Chem., 80, 905 (1976).
41. Leung, R. and Shah, D.O., Submitted to J. Colloid Interf. Sci.
42. Franks, F., "Physico-Chemical Processes in Mixed Aqueous Solvents", P. 63, American Elsevier Pub., N.Y. (1967).
43. Birdi, K.S., Backlund, S., Sorensen, K., Krag, T., and Dalsager, S., J. Colloid Interf. Sci., 66, 118 (1978).
44. Oakenfull, D., J. Colloid Interf. Sci., 88, 562 (1982).
45. Stilbs, P., J. Colloid Interf. Sci., 89, 547 (1982).
46. Dvolaitzky, M., Ober, R., Taupin, C., Anthore, R., Auvray, X., and Petipas, C., J. Dispersion Sci. & Tech., 4(1), 29 (1983).
47. Boutonnet, M., Kizling, J., Stenius, P., Colloids and Surfaces, 5, 209 (1982).

RECEIVED January 23, 1985